



Inertial Information Fusion for Improved Vehicular Perception Systems

Durdona Uktamova

Department of International Business Management, Tashkent State University of Economics, Uzbekistan

Email: d.uktamova@tsue.uz

Abstract

Advancing the capabilities of vehicle perception systems, through the fusion of sensor data is a pursuit in the field of vehicles and intelligent transportation systems. This study explores the complexities involved in enhancing vehicle perception with the goal of tackling the challenges associated with interpreting various sensor inputs to gain an understanding of the environment. By utilizing techniques that fuse information and clustering methodologies this research aims to identify driving scenarios based on patterns observed in sensor data allowing for a nuanced analysis of environmental variations. Additionally a classification framework using Convolutional Neural Networks (CNNs) is employed to accurately classify types of road surfaces demonstrating how deep learning models can effectively utilize sensor representations for environmental characterization. The methods employed encompass clustered data fusion, where K means clustering is utilized to segment sensor data into scenarios and CNN classification, for accurate identification of road surface types. The study achieved impressive findings using these methodologies, exhibiting unique clusters typical of various driving circumstances based on sensor aggregation and demonstrating the CNN's capacity for accurate road surface classification.

Keywords: Information Fusion; Inertial Data; Vehicular Perception; Machine Learning.

1. Introduction and background

The burgeoning advancements in vehicular technology have precipitated a paradigm shift in automotive safety, efficiency, and autonomy. Central to this evolution is the imperative enhancement of vehicular perception systems, which serve as the linchpin for vehicle awareness and decision-making [1-3]. Vehicular perception, the cognitive faculty enabling vehicles to interpret their surroundings, relies profoundly on sensor data amalgamation [4-7]. In this regard, the fusion of inertial information from various sensors has emerged as a pivotal approach, enabling vehicles to glean comprehensive and nuanced insights into their operational environment [8-11].

Inertial information fusion stands at the nexus of contemporary vehicular perception augmentation, leveraging data from inertial measurement units (IMUs) comprising accelerometers, gyroscopes, and magnetometers [12]. These sensors capture critical motion-related data, encompassing acceleration, angular velocity, and orientation, essential for deciphering a vehicle's kinematic state. Integrating this inertial data with inputs from other sensor modalities, such as LiDAR, radar, and cameras, presents a holistic perspective, mitigating the limitations inherent in individual sensor data streams. As vehicular technology evolves towards increased autonomy, the synergy achieved through inertial information fusion becomes pivotal for bolstering the perceptual capabilities requisite for safe and efficient navigation [13-16].

The efficacy of inertial information fusion lies in its capacity to mitigate sensor-specific drawbacks, thereby fortifying the reliability and accuracy of vehicular perception systems. Zhao et al. [14] conducted research on environmental perception and sensor data fusion for unmanned ground vehicles, highlighting the critical role of fused sensor data in

understanding and navigating complex terrains. By amalgamating disparate sensor data into a coherent representation of the vehicle's environment, this fusion technique transcends the limitations of singular sensors, mitigating issues such as environmental interference, sensor noise, and occlusion. Du et al. [15] proposed a real-time onboard 3D state estimation methodology for unmanned aerial vehicles, employing multi-sensor data fusion techniques to navigate various environments effectively. Consequently, the resultant fused data grants vehicles a more robust and comprehensive understanding of their surroundings, essential for critical decision-making processes, including collision avoidance, navigation in challenging terrains, and precise localization. Velasco-Hernandez et al. [16] provided an in-depth review of autonomous driving architectures, perception, and data fusion techniques, emphasizing the importance of robust fusion mechanisms for reliable autonomous vehicle operation.

Moreover, the evolution of inertial information fusion techniques underscores a pivotal stride towards enhancing vehicular perception beyond traditional paradigms. The synergistic amalgamation of inertial data with advancements in machine learning, artificial intelligence, and real-time processing engenders a transformative trajectory in the realm of vehicular perception. Cui et al. [17] presented an improved Simultaneous Localization and Mapping (SLAM) approach using the Runge-Kutta method, showcasing the efficacy of vision and inertial information fusion for precise localization in navigation systems. Fayyad et al. [18] offered insights into deep learning sensor fusion methodologies for autonomous vehicle perception and localization, highlighting the role of neural networks in integrating sensor data for enhanced decision-making. Polychronopoulos et al. [19] contributed to the domain of centralized data fusion for obstacle and road border tracking in collision warning systems, emphasizing the significance of centralized fusion techniques in enhancing vehicle safety systems.

2. Material and methods

This section delineates the foundational materials and methodologies employed in the pursuit of enhancing vehicular perception through inertial information fusion.

Algorithm 1: Gap Statistic

```

1: Input: X = sensors.load_data()
2: Output: k
3: def  $S_{Num}, P, Max_K, u, sigma$ ;
4:  $S_{Set} = []$ ;
5: size ( $u$ ) = [ $u$ ]
6: for  $i = 1: u$  do
7:    $S_{Set} = [S_{Set}, mvnrnd(u(i, :), sigma, fix(\frac{S_{Num}}{u}))]$ ;
8: end for
9:  $W_k = \log(\text{CompuW}(S_{Set}, Max_K))$ ;
10: for  $b = 1: P$  do
11:    $W_{kb} = \log(\text{Com}W_k(\text{RefSet}(\cdot, \cdot, b), Max_K))$ ;
12: end for
13: for  $k = 1: Max_K, Opt_K = 1$  do
14:    $Gap_k = (\frac{1}{P}) \sum_{b=1}^P \log(W_{kb}^*)$ ;
15:    $Gap_k \leq Gap_{k-1} + s(k), Opt_K == 1$ ;
16:    $Opt_K = k - 1$ ;
17: end for
18: return k

```

In our study section, we employed the K-means clustering algorithm as a pivotal technique for performing clustered data fusion. The objective was to amalgamate sensor data points into distinct clusters, thereby delineating patterns and associations within the dataset. This approach facilitated the categorization of data points into three principal clusters,

each representing unique vehicular scenarios based on combined sensor readings. Utilizing K-means clustering, we derived three distinct clusters:

First, Cluster 0 was characterized by high-speed instances coupled with low gyrometer readings. This cluster represented vehicular scenarios characterized by elevated velocity along with comparatively lower gyroscope sensor data. Second, Cluster 1 encompassed instances of low speed combined with low gyrometer readings and high magnetometer readings. This particular cluster denoted scenarios where vehicles operated at reduced speeds alongside concurrent low gyroscope readings and elevated magnetometer data. Third, Cluster 2 encapsulated instances of low speed coupled with high gyrometer and high magnetometer readings. This cluster delineated scenarios involving slower vehicular motion alongside heightened gyroscope and magnetometer sensor data.

To determine the optimal number of clusters for this data fusion process, we employed gap statistics. This statistical methodology enabled the assessment of clustering quality by evaluating the disparity between within-cluster variations for different cluster counts. The goal was to identify the optimal number of clusters that captured inherent structures within the dataset while avoiding overfitting or underfitting. This meticulous approach aided in ascertaining the most suitable number of clusters, ensuring a meaningful segmentation of the data into distinct vehicular scenarios based on the amalgamated sensor readings.

In our study, we extended our analytical approach beyond clustered data fusion to encompass a classification framework specifically tailored for road surface type identification. Here, we employed a Convolutional Neural Network (CNN) architecture, a deep learning model well-suited for image-based classification tasks, to discern and classify different road surface types based on sensor data representations.

The CNN was trained using a supervised learning approach, leveraging the amalgamated sensor data representations derived from the clustered fusion process. These representations encapsulated nuanced patterns and features characterizing various road surface types. By transforming the sensor data into a format akin to image inputs, the CNN model effectively learned discriminative features from the data, enabling robust classification of road surface types. Through this process, the CNN learned to discern subtle variations and patterns within the sensor data representations associated with asphalt, cobblestone, and dirt road surfaces. The network was trained to map these complex data representations to distinct classes corresponding to each road surface type. The model was fine-tuned iteratively, optimizing its ability to generalize and accurately classify road surface types unseen during training.

This approach not only allowed for the effective utilization of the amalgamated sensor data but also enabled the CNN to leverage its inherent ability to extract hierarchical and spatial features, effectively discerning distinct patterns indicative of different road surface types. The CNN classification framework served as a robust methodology for automated and accurate identification of road surface types based on sensor data representations derived from clustered fusion, contributing to a comprehensive understanding of the vehicular environment.

3. Experimental Design

This section outlines the systematic blueprint devised to rigorously evaluate the performance, accuracy, and robustness of the fusion framework in real-world scenarios.

For the experimental part of this study, a collection of nine distinct datasets is used, employing a range of sensors including GPS, cameras, inertial sensors (comprising accelerometers, gyroscopes), magnetometers, and temperature sensors. These datasets were meticulously generated to encompass contextual diversity across three key variables: vehicle type, driver identity, and environmental conditions. The experimental setup involved the deployment of hardware components, each strategically placed on the vehicles, as illustrated in the accompanying diagram. A roof-mounted camera and an internally positioned GPS receiver constituted the primary sensory apparatus. Additionally, two networks equipped with MPU-9250 modules were strategically distributed within the vehicles. These networks were affixed—one at each end of the front axle (right and left sides)—with one module situated beneath the vehicle's suspension system and another placed above, adjacent to the suspension system. A third module was installed inside the cabin, affixed to the vehicle's dashboard. To amass the nine Passive Vehicular Sensors Dataset (PVS) datasets, we employed multiple passive approach sensors for data collection, as outlined comprehensively in Table 1.

Table 1: Detailed configurations for our case study.

HP Webcam HD-4110	Camera	720p Video	30 Hz
MPU-9250	Accelerometer	3-axis acceleration in m/s ²	100 Hz
MPU-9250	Gyroscope	3-axis rotation rate in deg/s	100 Hz
MPU-9250	Magnetometer	3-axis ambient geomagnetic field in μ T	100 Hz
MPU-9250	Temperature	Sensor temperature in °C	100 Hz
Xiaomi Mi 8	GPS	Speed in m/s, latitude, longitude, etc.	1 Hz

The dataset acquisition process encompassed varied vehicular, driver, and environmental factors. Three different vehicles, driven by distinct individuals, traversed environments with divergent surface types. These environmental contexts exhibited variations in conditions, encompassing factors such as surface condition, presence of obstacles like speed bumps and potholes, and overall conservation state. This deliberate diversification ensured a comprehensive dataset capturing diverse real-world scenarios, facilitating a robust evaluation of vehicular perception systems. Table 2 details the data collection contexts.

Table 2: summary of details data collection in our case study.

DataSet	Vehicle	Driver	Scenario	Distance
PVS 3	Volkswagen Saveiro	Driver 1	Scenario 3	10.72 km
PVS 6	Fiat Bravo	Driver 2	Scenario 3	10.73 km
PVS 9	Fiat Palio	Driver 3	Scenario 3	10.74 km
PVS 2	Volkswagen Saveiro	Driver 1	Scenario 2	11.62 km
PVS 5	Fiat Bravo	Driver 2	Scenario 2	11.63 km
PVS 8	Fiat Palio	Driver 3	Scenario 2	11.63 km
PVS 7	Fiat Palio	Driver 3	Scenario 1	13.78 km
PVS 1	Volkswagen Saveiro	Driver 1	Scenario 1	13.81 km
PVS 4	Fiat Bravo	Driver 2	Scenario 1	13.81 km

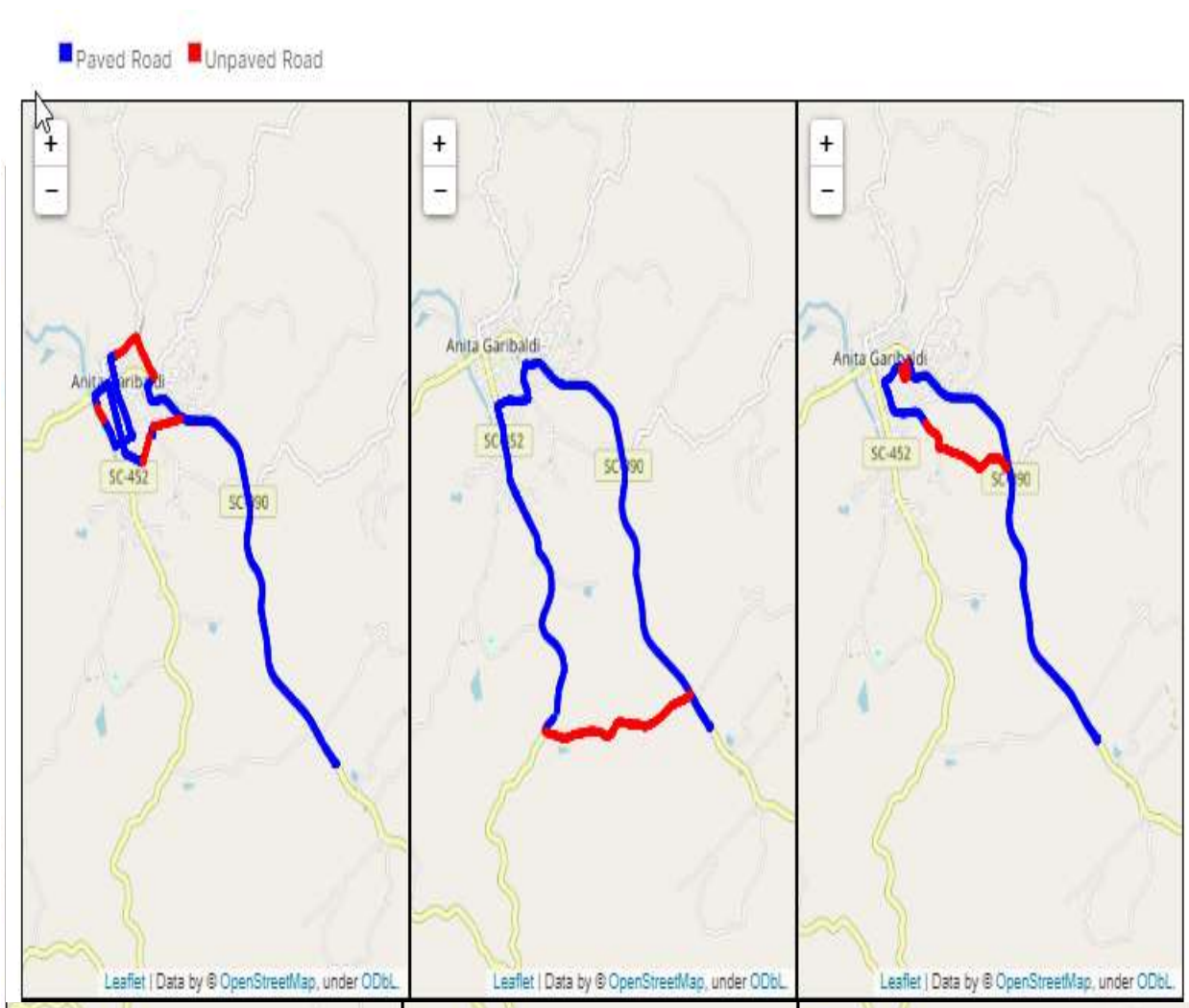


Figure 2: Visual of maps representation highlighting two distinct road surface conditions prevalent in the datasets

encountered in the datasets.

Figure 1 illustrates the distinct road surface types prevalent across the datasets, portraying asphalt, cobblestone, and dirt road surfaces. Each surface type denotes specific vehicular environments encountered during data collection, providing a visual representation of the diverse terrains navigated by the vehicles. The visualization highlights the variations in surface textures and composition, essential factors influencing vehicular performance and perception across different road surfaces.

In Figure 2, the visualization delineates the two primary road surface conditions encountered within the datasets: paved and unpaved roads. This depiction provides a clear differentiation between the two fundamental road conditions, encapsulating the varied states where vehicular perception systems operate. The visualization offers a comparative view, showcasing the distinct characteristics and challenges posed by paved and unpaved surfaces in vehicular navigation and perception.

Figure 3 offers an insightful portrayal of road roughness conditions prevalent in the datasets, showcasing three distinct levels: good, regular, and bad road surfaces. This visualization encapsulates the varying degrees of surface irregularities encountered during data collection, encompassing road roughness as a critical environmental factor. The visual representation aids in understanding the spectrum of road conditions, from smoother surfaces to significantly uneven terrains, crucial in assessing the adaptability and robustness of vehicular perception systems.

4. Results and Discussion

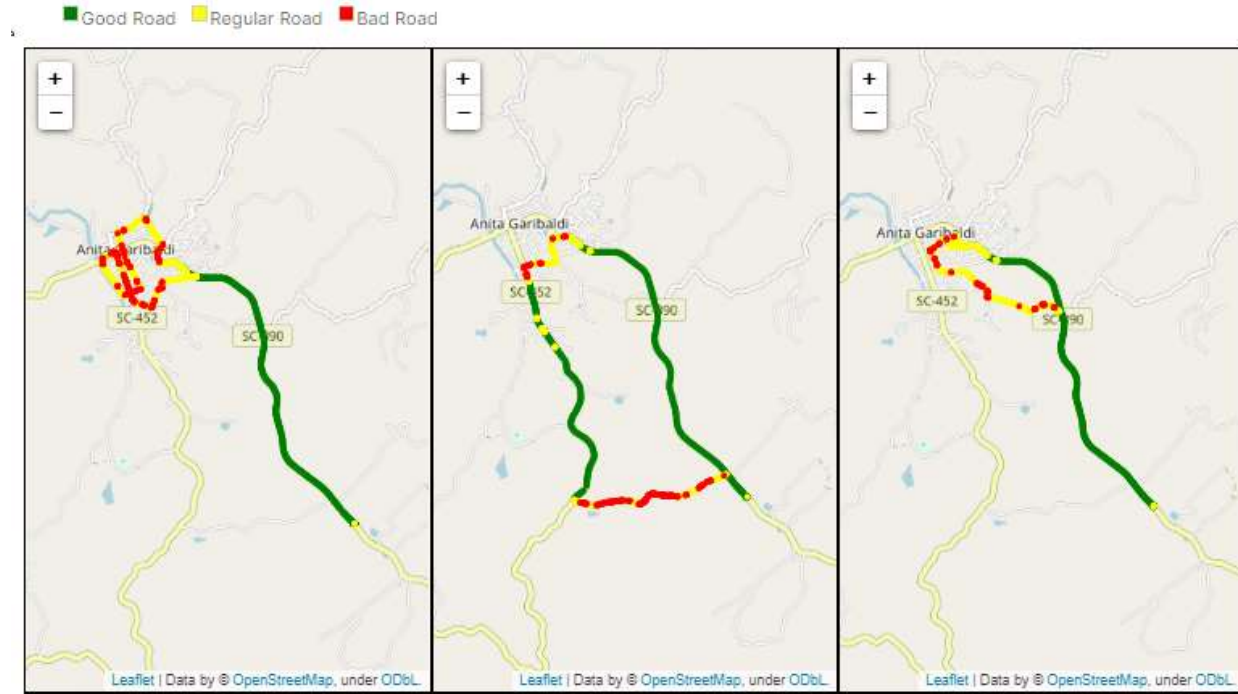


Figure 3: Visualization of maps showcasing three road roughness conditions—good, regular, and bad road surfaces—present in the datasets.

The culmination of meticulous experimentation and methodological rigor unfolds in this section, presenting the empirical outcomes and in-depth discussions derived from the fusion of inertial information within vehicular perception systems.

4.1. Statistical analysis

Table 3 encapsulates the results of the statistical analysis conducted on the dataset, presenting a comprehensive overview of key metrics and statistical parameters. This visualization aids in summarizing descriptive statistics, including mean values, standard deviations, and other relevant statistical measures across various dataset attributes. The tabulated statistical analysis offers a concise yet detailed representation, facilitating an understanding of the dataset's characteristics and distributions.

Table 3: Statistical analysis summary presenting key metrics and descriptive statistics.

	count	mean	std	min	25%	50%	75%	max
paved_road	144036	0.820406	0.38385	0	1	1	1	1
unpaved_road	144036	0.179594	0.38385	0	0	0	0	1
dirt_road	144036	0.179594	0.38385	0	0	0	0	1

cobblestone_road	144036	0.42808	0.494802	0	0	0	1	1
asphalt_road	144036	0.392326	0.48827	0	0	0	1	1
no_speed_bump	144036	0.976013	0.153009	0	1	1	1	1
speed_bump_asphalt	144036	0.004346	0.065782	0	0	0	0	1
speed_bump_cobblestone	144036	0.019641	0.138763	0	0	0	0	1
good_road_left	144036	0.392798	0.488374	0	0	0	1	1
regular_road_left	144036	0.453387	0.497824	0	0	0	1	1
bad_road_left	144036	0.153816	0.360773	0	0	0	0	1
good_road_right	144036	0.392923	0.488402	0	0	0	1	1
regular_road_right	144036	0.458483	0.498275	0	0	0	1	1
bad_road_right	144036	0.148595	0.35569	0	0	0	0	1

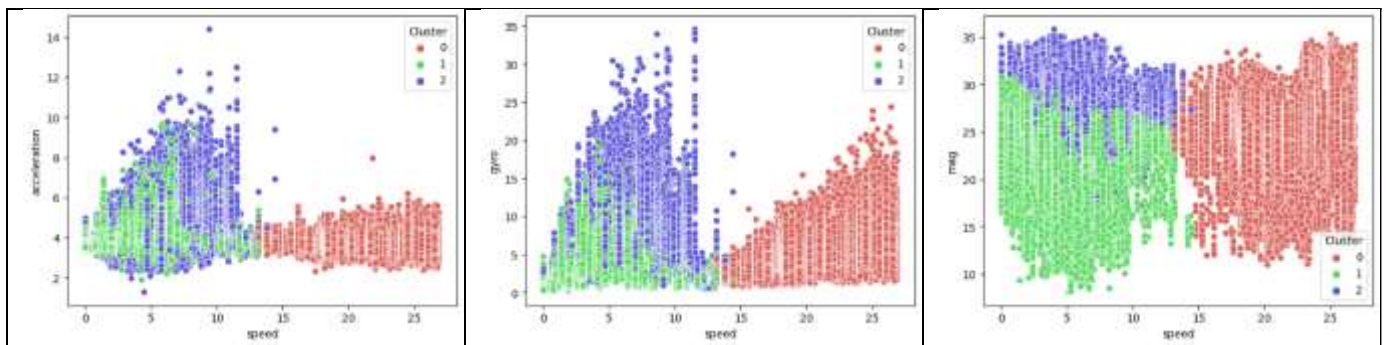


Figure 4: Visual representation showcasing the results of clustering analysis, revealing inherent data groupings or patterns identified within the dataset.

4.2. Clustering analysis

Figure 4 portrays the outcomes of the clustering analysis performed on the dataset, visually representing the clustered groupings or patterns discovered within the data. Through this visualization, distinct clusters or groupings of data points are depicted, highlighting inherent similarities or relationships among the dataset entities. This visual representation elucidates the efficacy of the clustering algorithm employed, providing insights into the inherent structures or associations present within the dataset. In Table 4, we show the classification report derived from the evaluation of a predictive model or classification system. This visual representation illustrates the performance of the model across different classes or categories. The classification report aids in assessing the model's accuracy, precision, recall, and other performance metrics, offering a clear depiction of the model's predictive capabilities and potential misclassifications among different classes within the dataset.

Table 4: Classification Report Summary presenting precision, recall, F1-score, and support for each class

	precision	recall	f1-score	support
Dirt Road	0.913777	0.976954	0.94431	998
Cobblestone Road	0.907738	0.794271	0.847222	384
Asphalt Road	0.991251	0.973368	0.982228	1164
accuracy	0.947761	0.947761	0.947761	0.947761
macro avg	0.937589	0.914864	0.924587	2546
weighted avg	0.948286	0.947761	0.947002	2546

5. Conclusion

This study presents a comprehensive exploration and application of sensor data fusion methodologies, culminating in the enhancement of vehicular perception systems. Through the amalgamation of diverse sensor inputs and the utilization of clustering techniques, we delineated distinct vehicular scenarios based on sensor data patterns, showcasing the potential for clustered data fusion to capture nuanced environmental variations. Moreover, the employment of a Convolutional Neural Network (CNN) for road surface type classification demonstrated the efficacy of deep learning models in discerning and classifying road surfaces based on sensor representations. These findings collectively underscore the significance of sensor data fusion in augmenting vehicular perception, paving the way for improved navigation, safety, and decision-making in diverse driving environments. However, while this study provides promising insights, further research avenues may delve into refining fusion techniques for real-time applications and expanding the classification framework to encompass a broader range of vehicular contexts.

References

- [1] Ounoughi, Chahinez, and Sadok Ben Yahia. 2023. "Data Fusion for ITS: A Systematic Literature Review." *Information Fusion* 89: 267–91.
- [2] Stiller, Christoph, Fernando Puente León, and Marco Kruse. 2011. "Information Fusion for Automotive Applications--An Overview." *Information Fusion* 12 (4): 244–52.
- [3] Seeliger, Florian, and Klaus Dietmayer. 2014. "Inter-Vehicle Information-Fusion with Shared Perception Information." In *17th International IEEE Conference on Intelligent Transportation Systems (ITSC)*, 2087–93.
- [4] Aeberhard, Michael, Stefan Schlichtharle, Nico Kaempchen, and Torsten Bertram. 2012. "Track-to-Track Fusion with Asynchronous Sensors Using Information Matrix Fusion for Surround Environment Perception." *IEEE Transactions on Intelligent Transportation Systems* 13 (4): 1717–26.
- [5] Morales, Joshua J, Joe J Khalife, and Zaher M Kassas. 2021. "Information Fusion Strategies for Collaborative Inertial Radio SLAM." *IEEE Transactions on Intelligent Transportation Systems* 23 (8): 12935–52.
- [6] Carmona, Juan, Fernando Garcí\`a, David Mart\`in, Arturo de la Escalera, and José Mar\`ia Armingol. 2015. "Data Fusion for Driver Behaviour Analysis." *Sensors* 15 (10): 25968–91.
- [7] Zhang, Xiaobin, Liangfei Xu, Jianqiu Li, and Minggao Ouyang. 2013. "Real-Time Estimation of Vehicle Mass and Road Grade Based on Multi-Sensor Data Fusion." In *2013 IEEE Vehicle Power and Propulsion Conference (VPPC)*, 1–7.
- [8] Liu, Ze, Yingfeng Cai, Hai Wang, Long Chen, Hongbo Gao, Yunyi Jia, and Yicheng Li. 2021. "Robust Target Recognition and Tracking of Self-Driving Cars with Radar and Camera Information Fusion under Severe Weather Conditions." *IEEE Transactions on Intelligent Transportation Systems* 23 (7): 6640–53.
- [9] Hoang, Gia-Minh, Beno\`it Denis, Jérôme Härrı, and Dirk T M Slock. 2017. "Robust Data Fusion for Cooperative Vehicular Localization in Tunnels." In *2017 IEEE Intelligent Vehicles Symposium (IV)*, 1372–77.
- [10] Khankalantary, Saeed, Sadra Rafatnia, and Hassan Mohammadkhani. 2020. "An Adaptive Constrained Type-2 Fuzzy Hammerstein Neural Network Data Fusion Scheme for Low-Cost SINS/GNSS Navigation System." *Applied Soft Computing* 86: 105917.

- [11] Li, Aijuan, Jiaping Cao, Shunming Li, Zhen Huang, Jinbo Wang, and Gang Liu. 2022. "Map Construction and Path Planning Method for a Mobile Robot Based on Multi-Sensor Information Fusion." *Applied Sciences* 12 (6): 2913.
- [12] Gruyer, Dominique, Rachid Belaroussi, and Marc Revilloud. 2014. "Map-Aided Localization with Lateral Perception." In *2014 IEEE Intelligent Vehicles Symposium Proceedings*, 674–80.
- [13] Dai, Minpeng, Haoyang Li, Jian Liang, Chunxi Zhang, Xiong Pan, Yizhuo Tian, Jinguo Cao, and Yuxuan Wang. 2023. "Lane Level Positioning Method for Unmanned Driving Based on Inertial System and Vector Map Information Fusion Applicable to GNSS Denied Environments." *Drones* 7 (4): 239.
- [14] Zhao, Yibing, Jining Li, Linhui Li, Mingheng Zhang, Lie Guo, and others. 2013. "Environmental Perception and Sensor Data Fusion for Unmanned Ground Vehicle." *Mathematical Problems in Engineering* 2013.
- [15] Du, Hao, Wei Wang, Chaowen Xu, Ran Xiao, and Changyin Sun. 2020. "Real-Time Onboard 3D State Estimation of an Unmanned Aerial Vehicle in Multi-Environments Using Multi-Sensor Data Fusion." *Sensors* 20 (3): 919.
- [16] Velasco-Hernandez, Gustavo, John Barry, Joseph Walsh, and others. 2020. "Autonomous Driving Architectures, Perception and Data Fusion: A Review." In *2020 IEEE 16th International Conference on Intelligent Computer Communication and Processing (ICCP)*, 315–21.
- [17] Cui, Jia-shan, Fang-rui Zhang, Dong-zhu Feng, Cong Li, Fei Li, and Qi-chen Tian. 2023. "An Improved SLAM Based on RK-VIF: Vision and Inertial Information Fusion via Runge-Kutta Method." *Defence Technology* 21: 133–46.
- [18] Fayyad, Jamil, Mohammad A Jaradat, Dominique Gruyer, and Homayoun Najjaran. 2020. "Deep Learning Sensor Fusion for Autonomous Vehicle Perception and Localization: A Review." *Sensors* 20 (15): 4220.
- [19] Polychronopoulos, Aris, Ullrich Scheunert, and Fabio Tango. 2004. "Centralized Data Fusion for Obstacle and Road Borders Tracking in a Collision Warning System." In *International Conference on Information Fusion*, 210–16.
- [20] Lytrivis, Panagiotis, Angelos Amditis, and George Thomaidis. 2009. "Sensor Data Fusion in Automotive Applications."
- [21] Liu, Long, Zhelong Wang, and Sen Qiu. 2020. "Driving Behavior Tracking and Recognition Based on Multisensors Data Fusion." *IEEE Sensors Journal* 20 (18): 10811–23.
- [22] Shi, Guolong, Yigang He, Bing Li, and Qiwu Luo. 2017. "Application of Multi-Sensor Information Fusion Based on Improved Particle Swarm Optimization in Unmanned System Path Planning." *International Journal of Online Engineering* 13 (8).
- [23] Wang, Peng, Xiangming Wen, Luhan Wang, Zhaoming Lu, and Lu Ma. 2019. "An Improved DS Based Vehicular Multi-Sensors' Perceptual Data Fusion for Automated Driving Decision-Making." In *2019 IEEE 90th Vehicular Technology Conference (VTC2019-Fall)*, 1–7.